Journal of Sound and Vibration 329 (2010) 1480–1498

Contents lists available at ScienceDirect

Journal of Sound and Vibration

journal homepage: www.elsevier.com/locate/jsvi

Proper orthogonal decomposition of the dynamics in bolted joints

Abdur Rauf Khattak [a,*], Seamus Garvey [b], Atanas Popov [b]

[a] 1569, Street 39, I-10/2, Islamabad 44000, Pakistan
[b] Department of Mechanical, Materials and Manufacturing Engineering, University of Nottingham, Nottingham, UK

ARTICLE INFO

Article history:
Received 21 April 2009
Received in revised form
11 September 2009
Accepted 13 November 2009
Handling Editor: L.G. Tham
Available online 6 December 2009

ABSTRACT

Joints play an important role in the dissipation of vibration energy in built-up structures. The highly nonlinear nature of joints with micro-slip is the main hurdle in developing a reduced-order model which can simulate the dynamic behaviour of a joint for a wide range of excitation conditions and geometries. In this paper, the proper orthogonal decomposition is applied to joint dynamics in an attempt to arrive at a generic reduced-order model without a compromise on the physics of the system. Only the linear part of the system of equations is reduced. The nonlinear part is determined in the full space and then reduced before the numerical integration phase. The major reduction in computational time is achieved by the increase in the size of the stable time step and the reduced number of coordinates in the integration phase. The reduced-order model, which is derived for an isolated and harmonically excited joint, is successfully applied to separate joints with different geometries and excitation conditions, e.g. harmonic and impulsive. The model is also capable of simulating the dynamics of structures with joints. The results of the reduced-order model show good agreement with a full model both in terms of the state of the system and its hysteretic behaviour.

1. Introduction

Joints, whether bolted or riveted, dissipate vibration energy through friction. Joints typically account for more than 90 percent of the total dissipated energy in fabricated structures [1]. Friction damping is a highly nonlinear phenomenon, especially when friction forces are comparable to the restoring forces in joints. Several approaches have been adopted to solve the nonlinear problem of friction damping. Metherell and Diller [2] have derived an analytical expression for the time history of the state of the joint with micro-slip and subjected to a single frequency harmonic excitation. According to this approach, the state of the joint is dependent on the past history of the micro-slip. Keeping track of this history is, however, cumbersome [3], especially when the forcing function contains harmonics of two or more frequencies [4]. The results of a detailed FE model have been utilised to determine the hysteretic behaviour of joints, [3,5,6], by utilising the so-called Jenkins element formulation. A very large FE model was developed at Sandia National Laboratory to reproduce the micro-slip behaviour of a joint using Coulomb friction [7]. The key parameters in these models, apart from the models given in [2] and [7], are obtained by curve fitting the response of a joint to known excitations [8,9]. It is, however, very difficult to reproduce the response of the same joint with these models when the frequency and/or the amplitude of the excitation is varied.

* Corresponding author. Tel.: +92 51 9257067.
E-mail address: rauf2@hotmail.com (A.R. Khattak).

0022-460X/$ - see front matter © 2009 Elsevier Ltd. All rights reserved.
doi:10.1016/j.jsv.2009.11.016

This study is aimed at developing a generalised joint model which should be capable of reproducing joint dynamics for a wide range of amplitudes and frequencies of excitation with only a few degrees of freedom (dofs). The model is based on the proper orthogonal decomposition (POD) of the time history of a representative joint. The POD is a method of extracting an optimal basis of spatially coherent structures, also known as proper orthogonal modes (POMs), from an ensemble of time histories resulting from numerical simulations or experiments [10]. The motivation to apply the POD to joint dynamics comes from the fact that joints are almost always excited by external forces and/or imposed displacements at the ends of the joint. This suggests the existence of some generic reduced order basis which should be capable of reproducing the state of the joint for a wide variety of excitation conditions. The analyses are, however, subjected to certain assumptions which are usually made when treating joint dynamics. These include: (1) there is no gross or macro-slip in the joint; (2) the excitation force and/or the imposed displacement act only at the free end of the joint; (3) clamping or normal force is distributed uniformly along the length of the joint; (4) there is no elastic compliance between the contacting surfaces; (5) the Coulomb formulation of friction force is used; and (6) the material behaves linearly.

It is also pertinent to mention that the model can easily be applied to structures with many shear lap joints. In that case the amplitude of the excitation force at each joint can be determined from the linear finite element (FE) analysis of the structure. This information will be utilised in properly scaling the POMs to reduce the nonlinear part of the structure. The linear part, of course, will require even lesser number generalised coordinates to fully simulate its behaviour. These generalised coordinates will depend on the frequency content of the excitation applied to the structure. The model will be applied to several complex aerospace structures in future. In this paper, however, application of the model is restricted to harmonic and impulsive excitations.

2. System description

The system under investigation is a simple shear lap joint made of two similar plates clamped together with a number of bolts causing a specified clamping pressure as shown in Fig. 1(a). The simplified representation of the joint for analysis purpose is shown in Fig. 1(b). It is reasonable to study the dynamics of joints based on the interaction of a deformable plate pressed against a rigid surface, as suggested e.g. in [3,4]. This approach has been adopted here as it offers simplicity and can be easily extended to the case of a joint having two deformable plates. It should be noted that the joint discussed here is first studied in isolation of the structure, so that a clearer understanding of the nonlinear dynamics of a bolted joint is gained. The structure of the joint is simulated by a simplified one dimensional FE model. The midpoint of the joint in Fig. 1(a) is selected as a reference point and a zero imposed displacement is assigned to it as shown in Fig. 1(b). A uniform pressure P is applied to the plate normal to the axial direction. Harmonic excitation, F_{exc} is applied at the free end while members of the friction force vector $\mathbf{f_f}$ act along the length of the plate.

As shear joints are designed to withstand longitudinal forces by friction rather than by bearing loads in through-bolts, it is assumed throughout this work that the joint will not fail and will always have certain nodes that will not see any relative displacement. This length in which nodes do not experience micro-slip is usually termed the 'grey' length as opposed to the 'active' length in which the nodes experiences micro-slip. The active length is also the maximum length experiencing micro-slip for a given excitation force. There can be both sticking and slipping regions in the active length while the grey length will have only sticking nodes and will remain unchanged for a given excitation condition.

2.1. Reference system

As a reference system, a plate of size $250 \times 50 \times 10$ mm is analysed with 100 strut elements along its length. The value of the friction coefficient is selected to be 0.7, while a uniform pressure of 8 MPa, equivalent to 100 kN of normal force,

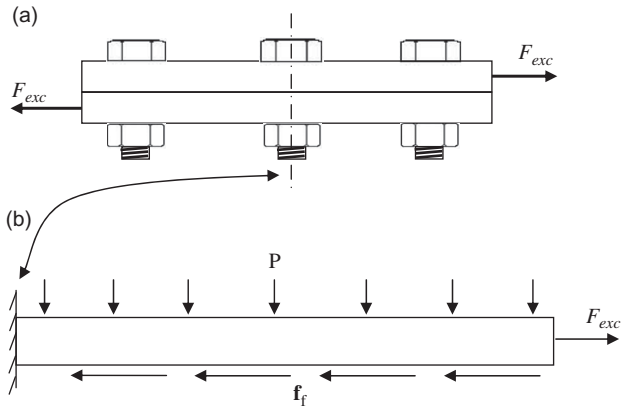

Fig. 1. Geometry of the joint: (a) actual isolated joint; and (b) its simplified model.

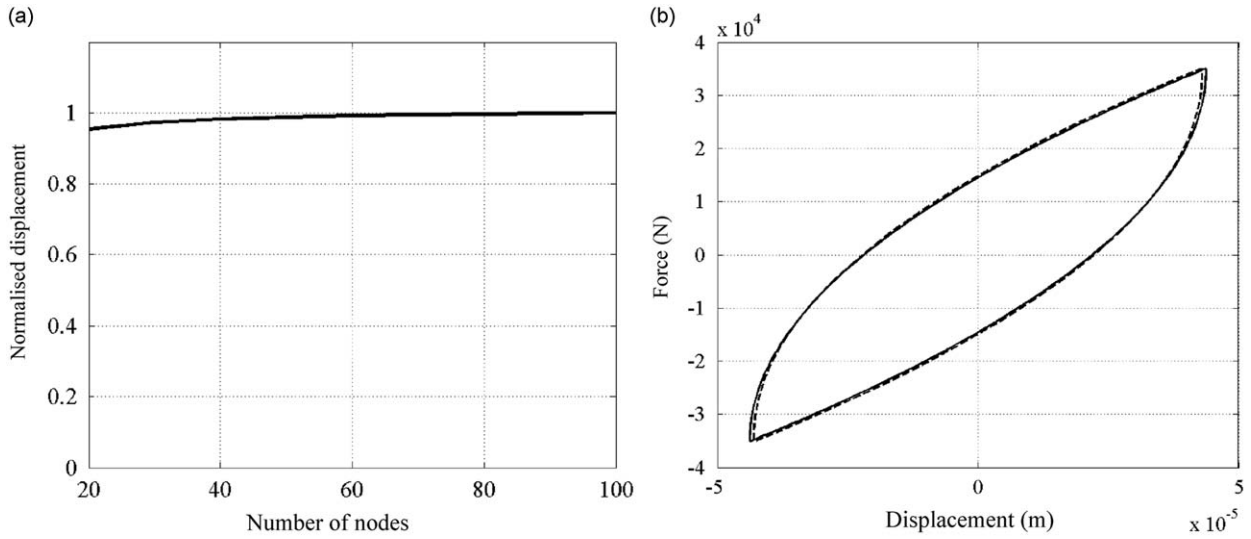

Fig. 2. Mesh sensitivity for displacement at the free end of the joint: (a) saturation of the displacement; and (b) comparison of a hysteresis curve with that of pseudo-static analytical approach [4] using 100 elements (both curves are almost overlapped).

is applied to the plate. A harmonic excitation force having amplitude of 63 kN at 1000 Hz is used which is 90 percent of the friction limit, i.e. 90 percent of 0.7×100 kN. This amplitude value causes a slip in almost 90 percent of the joint length which contains enough number of nodes to determine reasonably smooth POMs.

The FE model consists of one dimensional strut elements having consistent stiffness and mass matrix formulation [11]. The number of elements is selected on the basis of a mesh sensitivity study of the system and is found to be around 100 elements along the entire joint length. The mesh sensitivity is a direct consequence of the nonlinearity of the system. In the absence of nonlinear forces the same system dynamics can be modelled with fewer elements whose number is usually based on the frequency content of the excitation.

Fig. 2(a) shows the convergence of the value of displacement at the free end of the joint as a function of the number of elements for harmonic loading at 1000 Hz with amplitude equal to 90 percent of the friction limit of the joint. The plot in this figure shows a very small change, <1 percent compared with a model with a very large number of dofs, in the value of displacement at this level of refinement (100 elements). A comparison of the hysteretic behaviour of the system at this level of mesh refinement with the results of the pseudo-static system analysed analytically in [4] in Fig. 2(b) shows a very good agreement. The area enclosed by both curves, representing the energy dissipated per cycle, is equal to 2.0413 J.

3. Mathematical model

Dynamics of the joint model can be represented by the following system of equations:

$$\mathbf{Ku}+\mathbf{C}\dot{\mathbf{u}}+\mathbf{M}\ddot{\mathbf{u}}=\mathbf{f_{ln}}-\mathbf{f_f}. \tag{1}$$

Here **K**, **C** and **M** are the stiffness, viscous damping and mass matrices, respectively; **u** represents a vector of nodal displacements with a dot for derivatives with respect to time, $\mathbf{f_{ln}}$ is the vector of time dependant linear nodal excitation forces, while $\mathbf{f_f}$ is the vector of nonlinear nodal friction forces. **C** is assumed to be proportional to the stiffness matrix **K** and can be written as $\mathbf{C}=\varepsilon\mathbf{K}$, where $\varepsilon=10^{-5}$ is taken such as to accelerate convergence and to suppress contributions from higher resonances that are usually not of interest in mechanical systems.

The nonlinear Coulomb friction force vector, $\mathbf{f_f}$, which is governed by a sign function of the velocity, is represented by the inverse tangent function to avoid a discontinuous friction force variation. It can be written, following [12], as

$$\mathbf{f_f}=\mu f_N\left(\frac{2}{\pi}\tan^{-1}(\beta\dot{\mathbf{u}})\right). \tag{2}$$

Here μ is the coefficient of friction with the assumption that static and kinetic friction coefficients are equal, f_N is the normal force per node and β is a scalar that governs the slope of the curve representing the variation of friction force with $\dot{\mathbf{u}}$, where $\dot{\mathbf{u}}$ is the vector of relative velocities between the rigid surface and the contacting nodes. A plot of normalised inverse tangent function against $\dot{u}$, where $\dot{u}$ is some nodal velocity, is shown in Fig. 3.

At lower excitation frequencies, resulting in lower nodal velocities for the same displacements, this factor should be increased accordingly but this leads to increase in computational time. This is evident from Fig. 4 in which a comparison of nodal displacements at the free end of the joint is given for two different values of the excitation frequency and two different values of β. Fig. 4(a) shows that for a frequency of excitation equal to 5 Hz the change in displacement can be as

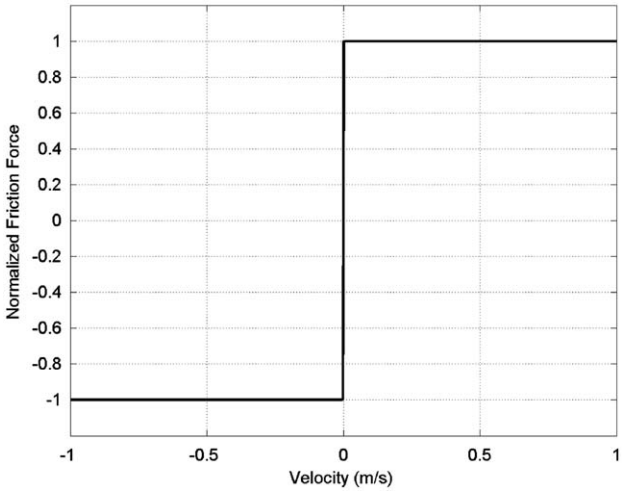

Fig. 3. Variation of the friction force with velocity using the arctan function.

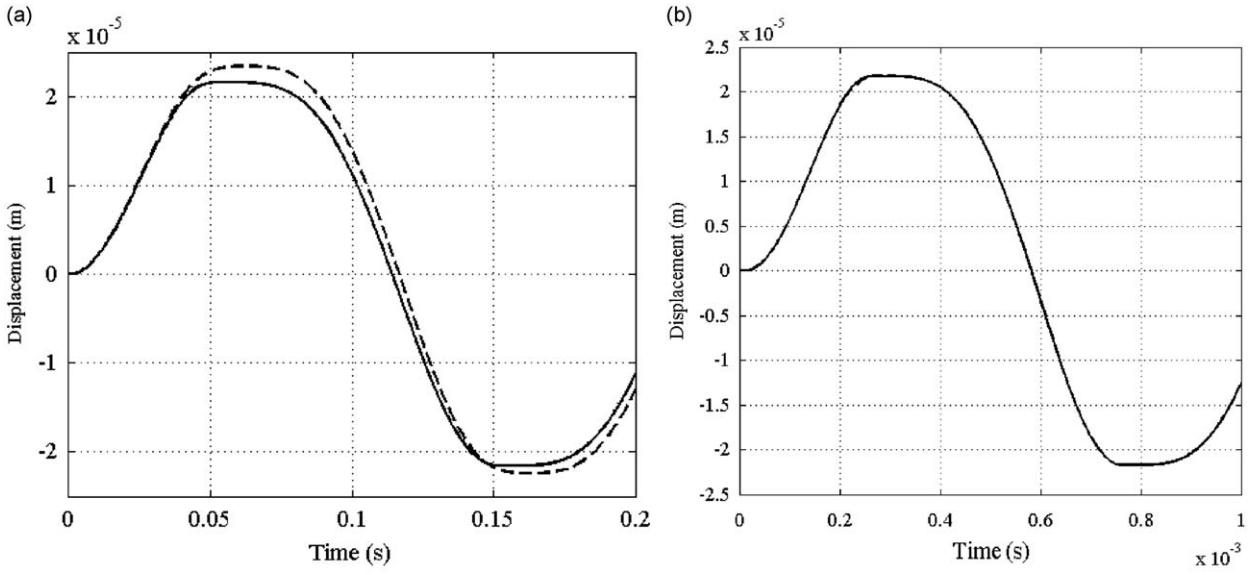

Fig. 4. Effect of the scaling constant β in Eq. (2), on the response of the joint: (a) f_{exc}=5 Hz and (b) f_{exc}=1000 Hz for β=10^7 (solid) and β=10^5 (dashed) (both curves are overlapped (b)).

large as 9 percent when the value of β is increased from 10^5 to 10^7. Fig. 4(b) shows the corresponding change for excitation frequency equal to 1000 Hz and is <1 percent. The computational time is also increased several times for this change in the value of β.

4. POD of joint dynamics

The POD is closely related to the eigenvalue factorisation of a symmetric matrix [13] with the difference that the POD can be applied to rectangular matrices as well. The time history of nodal displacements $\{\mathbf{u}(t)\}_{p\times n}$, where p is the number of time steps and n is the number of nodes in the joint, is determined by numerical integration using (1) for the reference system. Using the POD, the matrix of nodal displacements is decomposed according to the following equation:

$$\{\mathbf{u}(t)\}_{p\times n} = \mathbf{U}_{p\times p}\mathbf{\Sigma}_{p\times n}\mathbf{V}^{\mathbf{T}}_{n\times n}. \tag{3}$$

Here '**T**' in the exponent means transposition, **U** and **V** are orthogonal square matrices of size p and n, respectively. $\mathbf{\Sigma}$ is a diagonal but rectangular matrix having singular (proper) values $\sigma_1, \sigma_2, \ldots, \sigma_n$ at its main diagonal. The columns of **V** are the

POMs corresponding to the PVs $\sigma_1, \sigma_2, \ldots, \sigma_n$ satisfying the orthogonality property $\mathbf{v}_i^{\mathbf{T}}\mathbf{v}_j = \delta_{ij}$, where δ_{ij} is the Kronecker delta. It should be noted that the entries in the columns of $\mathbf{V}$ corresponding to the grey region are all zero. The matrix $\mathbf{V}$ contains the eigenvectors of the dot product $\{\mathbf{u}(t)\}_{p\times n}^{\mathbf{T}}\{\mathbf{u}(t)\}_{p\times n}$, corresponding to the eigenvalues $\lambda_1, \lambda_2, \ldots, \lambda_n$ such that $\sigma_i^2 = \lambda_i$ while $\mathbf{U}$ is the matrix of eigenvectors for $\{\mathbf{u}(t)\}_{p\times n}\{\mathbf{u}(t)\}_{p\times n}^{\mathbf{T}}$. The factorisation in (3) can be obtained by a standard function, e.g. in MATLAB, the *svd* command [14].

The scaled and normalised PVs corresponding to the first five POMs for the reference system are given in Table 1 and the first five corresponding POMs are shown in Fig. 5(a). The scaling in Table 1 is done by dividing the PVs obtained from (3) with their sum and by multiplying the result by 100. The value of the cumulative sum in the third column in Table 1 for the i-th POM is obtained by adding the first i values in the second column of this table. The POMs have zero amplitude and slopes at the interface of the active and grey regions. The zero value of the abscissa in Fig. 5(a) corresponds to this interface. The active length of the joint is normalised to unity and the amplitude of the POMs is plotted against this length.

Since in most cases the joint experiences excitations at its extreme ends in the form of applied forces or imposed displacements it is natural to think that the behaviour of the POMs for different values of the excitation amplitude and frequency will have some commonality. To check whether this is true, the POD is applied to another system which has the same geometry as the reference system but with smaller excitation amplitude, i.e. 28 kN, at 100 Hz. This value corresponds to 40 percent of the friction limit of the joint. The POMs of the time history of this system are plotted in Fig. 5(b). Reasonable number of time steps, around 100 for one time period, is taken to obtain this time history. Although the excitation amplitude and frequency are different for the two systems in Fig. 5, the POMs resemble each other very closely.

Although Fig. 5 shows the resemblance between POMs obtained for different systems, their quantitative behaviour needs some clarification. The amplitude of the POMs in Fig. 5(a) is small compared with those in Fig. 5(b). The amplitude of the POMs for the second case (Fig. 5(b)) can be obtained by dividing the amplitude of the POMs of the reference system with the square root of the ratio of the excitation amplitudes, i.e. the square root of the ratio of 28 kN (40 percent of the friction limit) and 63 kN (90 percent of the friction limit). The interested reader is referred to [15] for a detailed description of the quantitative behaviour of the POMs.

Table 1
Proper values (PVs) and their cumulative sum for the reference case.

No.	POD of displacement	
	Proper values	Cumulative sum
1	86.55	86.55
2	10.24	96.79
3	1.70	98.49
4	0.73	99.22
5	0.29	99.51

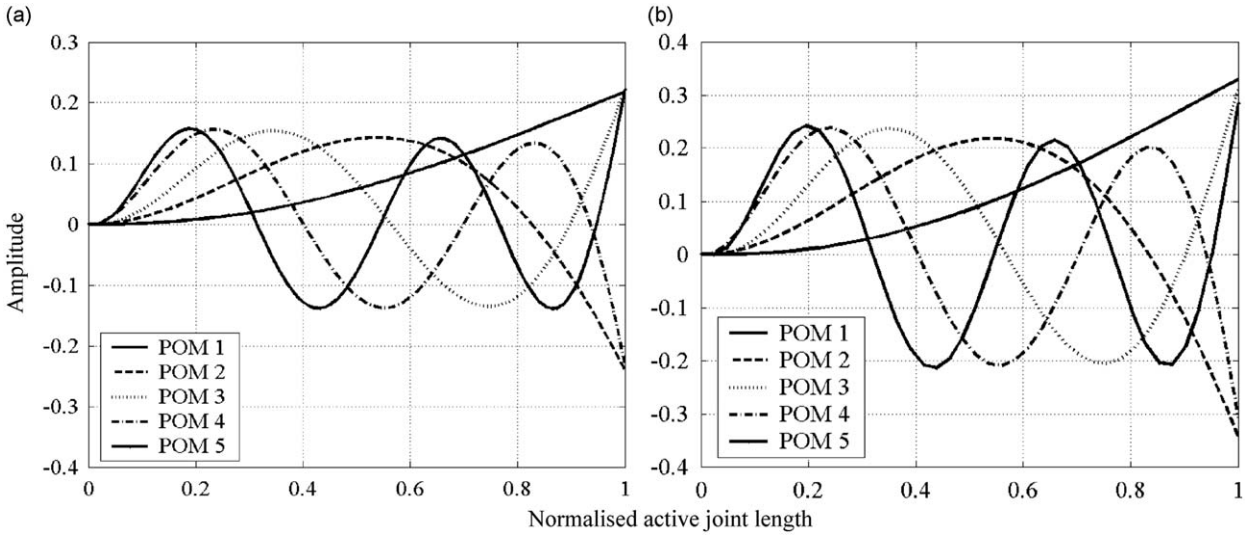

Fig. 5. The first five POMs for: (a) the reference system; and (b) reference system with excitation amplitude equal to 40 percent of joint friction limit.

5. Reduction of the joint model

Assume for a moment that the grey and active lengths of the joint are known (this will be made clear in Section 6), the transformation matrix $\mathbf{V}$ is constructed such that the entries in its columns corresponding to the grey region are all zero and the POMs are adjusted to the active region only. This transformation matrix is now applied to transform the system equations, Eq. (1), using the first j columns of $\mathbf{V}$. The first columns of $\mathbf{V}$ are selected as they correspond to the larger PVs. (The PVs are arranged in decreasing order).

Defining $\mathbf{V}_1 = \{\mathbf{v}_1\mathbf{v}_2\mathbf{v}_3 \ldots \mathbf{v}_j\}$, where $\mathbf{v}_j$ are the first j columns of $\mathbf{V}$ and $j \le n$, with $\mathbf{u} = \mathbf{V}_1\mathbf{u}'$ in (1) and pre-multiplying this equation by $\mathbf{V}_1^{\mathbf{T}}$ results in the following reduced system of equations:

$$\mathbf{K}'\mathbf{u}' + \mathbf{C}'\dot{\mathbf{u}}' + \mathbf{M}'\ddot{\mathbf{u}}' = \mathbf{f}'_{\mathbf{ln}} - \mathbf{f}'_{\mathbf{f}}, \tag{4}$$

where

$$\mathbf{K}' = \mathbf{V}_1^{\mathbf{T}}\mathbf{K}\mathbf{V}_1, \tag{5}$$

$$\mathbf{C}' = \mathbf{V}_1^{\mathbf{T}}\mathbf{C}\mathbf{V}_1, \tag{6}$$

$$\mathbf{M}' = \mathbf{V}_1^{\mathbf{T}}\mathbf{M}\mathbf{V}_1, \tag{7}$$

$$\mathbf{f}'_{\mathbf{ln}} = \mathbf{V}_1^{\mathbf{T}}\mathbf{f}_{\mathbf{ln}} \tag{8}$$

and

$$\mathbf{f}'_{\mathbf{f}} = \mathbf{V}_1^{\mathbf{T}}\mathbf{f}_{\mathbf{f}}. \tag{9}$$

These equations are straightforward except for (9) which is responsible for the nonlinear behaviour of the system. A reasonable value of j is normally selected based on the cumulative sum of the PVs. As a general rule, this value is taken to be 99 percent of the total sum of PVs. In this analysis the first five POMs are selected to reduce the system of equations although the cumulative sum of the corresponding PVs is slightly more than 99 percent, as can be seen from Table 1. Because the PVs can change slightly when varying the excitation conditions, the number of POMs is one higher than is strictly indicated by the 99 percent criterion.

Eqs. (1) and (4) are usually solved using the state-space formulation. This method results in a system of first-order equations that is double the size of the original system of second-order equations. The method assumes two new vectors say $\mathbf{y}_1$ and $\mathbf{y}_2$ each of size $n \times 1$ such that $\mathbf{y}_1 = \mathbf{u}$ and $\mathbf{y}_2 = \dot{\mathbf{u}}$ i.e. $\mathbf{y}_1$ is the displacement vector and $\mathbf{y}_2$ is the velocity vector of the original system. This means that

$$\dot{\mathbf{y}}_1 = \dot{\mathbf{u}} = \mathbf{y}_2 \tag{10}$$

and

$$\dot{\mathbf{y}}_2 = \ddot{\mathbf{u}} = -\mathbf{M}^{-1}(\mathbf{K}\mathbf{u} + \mathbf{C}\dot{\mathbf{u}} - \mathbf{f}_{\mathbf{ln}} + \mathbf{f}_{\mathbf{f}}). \tag{11}$$

These two equations result in the following first-order equation:

$$\dot{\mathbf{y}} = \mathbf{A}\mathbf{y} + \mathbf{b}, \tag{12}$$

with $\mathbf{y} = \{\mathbf{y}_1 \ \ \mathbf{y}_2\}^{\mathbf{T}}$, where

$$\mathbf{A} = \begin{bmatrix} \mathbf{0}_{n\times n} & \mathbf{I}_{n\times n} \\ -\mathbf{M}^{-1}\mathbf{K} & -\mathbf{M}^{-1}\mathbf{C} \end{bmatrix} \tag{13}$$

and

$$\mathbf{b} = \begin{Bmatrix} \mathbf{0}_{n\times n} \\ \mathbf{M}^{-1}(\mathbf{f}_{\mathbf{ln}} - \mathbf{f}_{\mathbf{f}}) \end{Bmatrix}. \tag{14}$$

For the reduced system $\mathbf{y}_1 = \mathbf{u}'$, $\dot{\mathbf{y}}_1 = \dot{\mathbf{u}}' = \mathbf{y}_2$ and matrix $\mathbf{A}$ and vector $\mathbf{b}$ are given by

$$\mathbf{A} = \begin{bmatrix} \mathbf{0}_{k\times k} & \mathbf{I}_{k\times k} \\ -\mathbf{M}'^{-1}\mathbf{K}' & -\mathbf{M}'^{-1}C' \end{bmatrix} \tag{15}$$

and

$$\mathbf{b} = \begin{Bmatrix} \mathbf{0}_{k\times k} \\ \mathbf{X}(\mathbf{f}_{\mathbf{ln}} - \mathbf{f}_{\mathbf{f}}) \end{Bmatrix}, \tag{16}$$

where $\mathbf{X} = \mathbf{M}'^{-1}\mathbf{V}_1^{\mathbf{T}}$.

For the reduced system, the velocity vector $\dot{\mathbf{u}}'$ has to be expanded at each time step to the full velocity vector using $\dot{\mathbf{u}} = \mathbf{V}_1\dot{\mathbf{u}}'$ in order to determine the nonlinear friction force vector according to (2). This expansion of reduced solution to the full one for obtaining the full nonlinear force vector and then the compression of nonlinear force vector to the reduced

one in (16) gives rise to additional computational cost at each time step. In spite of this drawback the method results in computational savings, for the number of modes used in the analysis is much smaller when compared with the full size of the system.

6. Active length of the joint

It is mentioned before that the nodal displacements in the grey length only remain zero at all times. This suggests that the POD should be applied to the dynamics of the active region only, i.e. the POMs should be scaled according to this length. It is, therefore, natural to determine the active length of a joint before embarking on the decomposition of the dynamics of the system.

A number of simulations have been performed to check if the active length can be determined beforehand at different frequencies including the internal resonance. The inertia forces of a dynamical system, which are dependent on the frequency of excitation when keeping other factors unchanged, become predominant in the vicinity of a system resonance. This tends to increase the active length of a joint and means that if the applied force is scaled properly to include the inertia effects, the active length of the joint can be determined correctly. The dependence of the active length on the frequency content of the harmonic and impulse excitation forces is discussed in this section.

For the case of multi-harmonic excitation, the active length will be determined using the superposition principle, i.e. contributions from all the harmonics will be added at a point in time and the resulting maximum amplitude will be used to determine the active length. This treatment is, however, not included in this paper.

6.1. Harmonic excitation

It is well known that the response of a linear SDOF system is amplified by the factor

$$A_a = \frac{1}{\sqrt{(1-r_\omega^2)^2+(2r_\omega\zeta)^2}}, \tag{17}$$

where $r_\omega = \omega/\omega_n$, ω is the excitation frequency, ω_n is the undamped resonance frequency and ζ is the damping ratio for the mode having ω_n as natural frequency. This is, however, not true for nonlinear systems especially bolted joints for which ω_n is a function of both excitation frequency and amplitude. An iterative procedure is adopted to arrive at a plausible value for the scaling factor A_a. According to this procedure ω_n is first determined on the basis of the amplitude of excitation at a given value of ω. The value of the factor A_a is calculated from the initial value of ω_n. This factor is then applied to scale the active length δ_a. The increased active length reduces the natural frequency ω_n which in turn increases the factor A_a. After a few iterations a converged value of the scaling factor can be achieved. The value of the damping ratio ζ is determined following the pseudo-static approach adopted in [4]. The term pseudo-static is used because the inertial effects of the joint are ignored in this study although the excitation force is time dependant. According to this study the equivalent stiffness and damping of a joint, having an active length equal to δ_a, can be written as

$$k_{eq} = \frac{2EA_x\sqrt{(9\pi^2-16)}}{3\pi\delta_a} \tag{18}$$

and

$$c_{eq} = \frac{8EA_x}{3\pi\delta_a\omega}. \tag{19}$$

These relations were derived analytically by modelling the joint with first-order differential equation and thus ignoring the inertia effects. The value of c_{eq} is determined by equating the energy dissipated per cycle in the joint to that of a viscously damped system based on a commonly adopted linearisation approach. The value of k_{eq} is then determined from the first-order differential equation of the joint model. Eq. (18) shows that $k_{eq}\to\infty$ as the active length $\delta_a\to 0$, an obvious conclusion that the stiffness of a strut with infinitesimal extendible length approaches infinity.

The loss factor η and hence the damping ratio ζ can now be determined, following [16], as

$$\zeta = \frac{\eta}{2} = \frac{c_{eq}\omega}{2k_{eq}} = \frac{2}{\sqrt{(9\pi^2-16)}} = 0.234. \tag{20}$$

It is evident that the equivalent stiffness and damping are inversely proportional to the active length of the joint and the loss factor and the damping ratio are independent of the active length.

As an example the typical converging behaviour of the scaling factor A_a for Case I (Table 2) at 2000 Hz is shown in Fig. 6. In this example $\omega_n = 2\times\pi\times 5000$ rad/s, $\omega = 2\times\pi\times 2000$ rad/s, hence $r_\omega = 0.4$ and $A_a = 1.162$. New value of the active length comes out to be $0.25\times 1.162 = 0.2905$ mm and hence the new $\omega_n = 2\times\pi\times 4303$ rad/s. After 15 iterations the converged value of 1.3 is achieved.

Three cases are investigated to check the dependence of the active length on the excitation frequency. Parameter values for these cases are given in Table 2. The first two cases are selected to determine the active length for different values of the

Table 2
System parameters used for the determination of active length of the joint in Fig. 1.

Parameter	Case I	Case II	Case III
Joint length (mm)	500	250	500
Plate thickness (mm)	10	10	10
Plate width (mm)	50	50	50
Normal pressure (MPa)	50	50	50
Normal force (kN)	1.25×10^3	6.25×10^2	1.25×10^3
Friction coefficient	0.7	0.1	0.1
Excitation amplitude (kN)	437.5	31.25	37.5
First internal resonance (Hz)	5000	10 000	8333

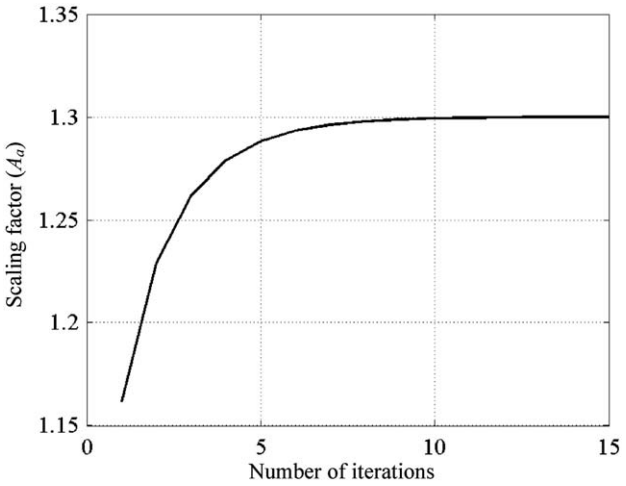

Fig. 6. Convergence of scaling factor A_a.

friction coefficient keeping the amplitude of excitation equal to 50 percent of the friction limit. The third case is chosen to determine the active length for a smaller value of the excitation amplitude, 30 percent of the friction limit. Results for these cases are shown in Fig. 7. The plots in this figure show the variation of the active length with the frequency of excitation. The locations of the resonances of the systems are marked with arrows in these plots and the active length is taken as a percentage of the joint length. The first (solid) curve in these plots show the results of the full FE analysis of the problem while the second (dashed) curve show the active lengths determined by the above developed procedure using the POMs of the reference system.

Fig. 7 shows a good agreement between the actual active length obtained from the full FE analysis of the problem and the scaled active length for values of the excitation frequencies outside, up to 50 percent, of the internal resonance of the system. The error in active length in Figs. 7(a), (b) and (c) is 3.2 percent, 1.8 percent and 5.9 percent, respectively, at about 50 percent of the internal resonance. The relatively large error in Fig. 7(c) is a result of the smaller number of elements in the active length of the joint. The increase in the error at frequencies more than 50 percent of the internal resonance is a result of the assumptions made in the determination of the effective stiffness and damping. The values of k_{eq} and c_{eq} are determined by linearisation of the hysteretic curve which is obtained by ignoring the inertia effects on the system. It is, however, very difficult to derive such simple relations for k_{eq} and c_{eq} when the inertia of the system is included in the formulation of the problem.

It should, however, be noted that this discussion relates to the dependence of the active length of an isolated joint on its internal resonance. In real structures, the resonance of the whole structure is important and which is usually quite lower than the resonance of the joint. Hence the error in the value of the scaled active length, in general, will be smaller.

Fig. 8 shows the harmonic response histories at the free end, obtained from the full, reduced, pseudo-static and scaled pseudo-static analysis. In the scaled pseudo-static analysis, the amplitude is obtained by scaling the pseudo-static response with factor A_a. The system in Case I is selected for this analysis with the excitation frequency and amplitude equal to 2000 Hz and 50 percent of the friction limit. This value of excitation frequency is large enough for the inertia forces to be included, while at the same time it is kept reasonably below the point where the amplification factor, A_a, does not give correct value of the active length. Only the steady-state part of the response is shown in this figure as the pseudo-static approach does not account for the transient behaviour at the beginning of the simulation. The time history from the

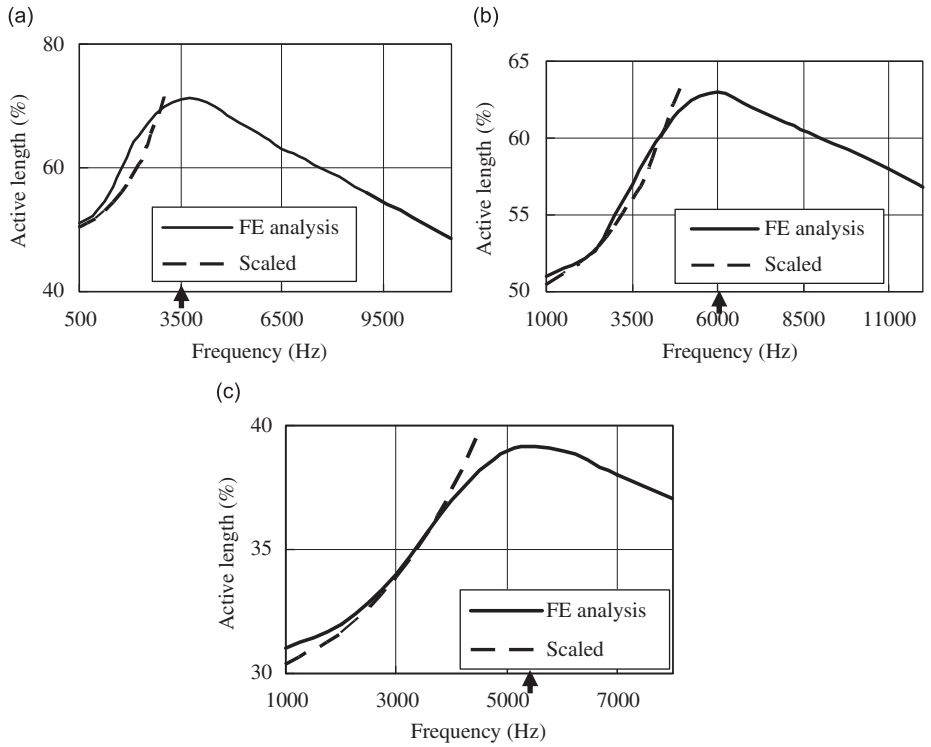

Fig. 7. The variation of active length (percent of total) with excitation frequency for different amplitudes of excitation for: Case I (a); Case II (b); and Case III (c). The abscissa location marked with arrow shows the resonance of the system.

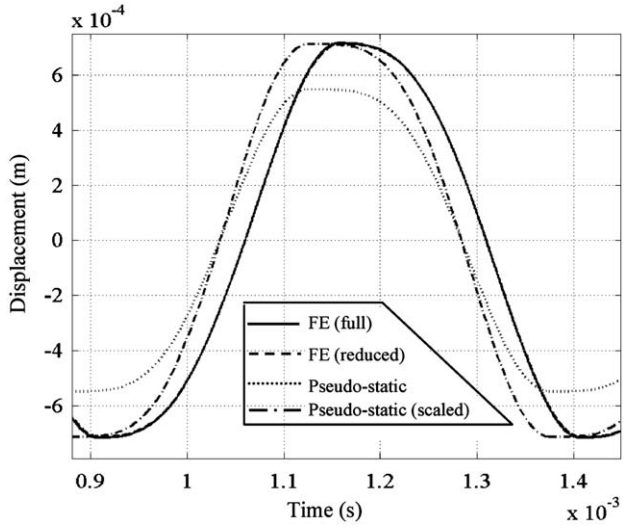

Fig. 8. Comparison of the displacement at the free end of the joint for the full, reduced, pseudo-static and scaled pseudo-static analysis (full and reduced FE plots are overlapped).

pseudo-static analysis (dotted) and its scaled values (dashed-dotted) by applying Eq. (17) are also plotted in Fig. 8. Some representative values of the results of these analyses are given in Table 3. The values in parentheses in Table 3 are the errors compared with the full FE analysis. These values show that the reduced solution based on the scaled active length agrees well with the full solution. Finally the hysteresis curves corresponding to the time histories in Fig. 8 are plotted in Fig. 9. These show the accuracy of the method developed in this paper. This figure also indicates the limitation of the pseudo-static approach at higher frequencies of excitation.

Table 3
Comparison of results of the dynamic and pseudo-static analyses based on scaling of the active length (Figs. 8 and 9).

Analysis type	Max. displacement (m)	Energy/cycle (J)
Dynamic FE analysis (full)	7.14×10^{-4} (0%)	681 (0%)
Dynamic FE analysis (reduced)	7.10×10^{-4} (0.6%)	680 (0.2%)
Pseudo-static [4]	5.47×10^{-4} (23.4%)	319 (53.2%)
Scaled pseudo-static	7.11×10^{-4} (0.4%)	415 (39.1%)

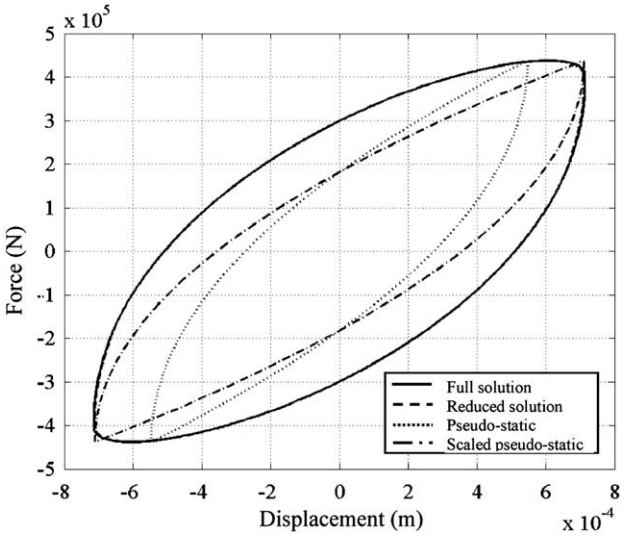

Fig. 9. Hysteresis curves corresponding to Fig. 8, full system (solid line), reduced (dashed), pseudo-static (dotted) and scaled pseudo-static (dashed-dotted) (full and reduced solutions are overlapped).

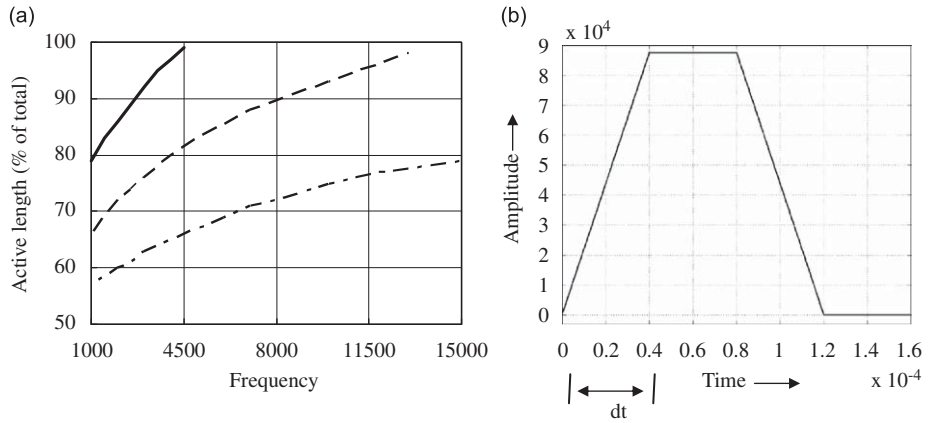

Fig. 10. (a) Variation of active length for impulsive excitation with the maximum frequency content of the excitation for load amplitudes equal to 70 percent (full), 60 percent (dashed) and 50 percent (dashed-dotted) of the joint friction limit; and (b) a representative impulsive excitation.

6.2. Impulsive excitation

The determination of the active length in the case of impulse excitation is even more complicated when compared to the case of harmonic excitation. The complexity is due to the fact that the change in the amplitude of the excitation force is discontinuous and that the excitation is rich in frequencies when compared with the harmonic case.

The dynamic system of Case I is selected for this study and the active length of the joint for various loading amplitudes is plotted against maximum frequency, present in the impulsive excitation, in Fig. 10(a). The corresponding impulse is shown in Fig. 10(b). The maximum frequency present in the excitation can be found from dt in Fig. 10(b) using Nyquist

rule. The three different curves in this figure correspond to three different amplitudes of the impulse. This figure shows that the active length for one level of excitation can be scaled with the ratio of the amplitudes to obtain its value at another level of excitation. For example, the value of the active length for amplitude of the impulse equal to 50 percent of the friction limit at 4500 Hz is 66 percent of the joint length. When this value of the active length is scaled for a load level equal to 70 percent of the friction limit, it comes out to be $70/50 \times 66 = 92$ which is quite close to the actual value at this level of excitation which is 99 percent of the joint length. The error in the scaled value of the active length is therefore 7 percent. The sensitivity of the response to the error in the value of the active length is discussed in the next section.

Although it is possible to relate the values of the active length for different amplitudes of the impulse having the same maximum frequency for a given case, it is not very easy to reach at any general conclusion about the frequency dependence of the active length for this kind of excitation.

6.3. *Sensitivity of the response to the value of the active length*

Sensitivity of the response to the active length of the joint is investigated by the application of a harmonic excitation to the structure in Case I. The frequency of excitation is selected at 2000 Hz which is about 50 percent of the first internal resonance. The amplitude of excitation is selected as 50 percent of the friction limit. This amplitude suggests that the active length, without taking into account the inertia effects, is 50 percent of the joint length, i.e. 250 mm. The first resonance of the structure in Case I having a length of 250 mm is 5000 Hz. The active length comes out to be 345 mm when the inertia effects are included according to (17). Results using this length for the reduced model are already reported in Table 3 and Fig. 8.

To check the sensitivity of the response to change in the value of active length, two simulations are carried out. In the first one the active length obtained from the analysis of the full model is increased by 10 percent while in the second one it is reduced by 10 percent. Fig. 11(a) shows the response histories while Fig. 11(b) shows the hysteresis behaviour. The representative values of the results of these analyses are given in Table 4 which is very encouraging as the maximum error in response and/or energy dissipated per cycle is around 2 percent. This is due to the fact that the amplitude of the POMs is small at the junction of the grey and active length. A small change in the value of the active length, therefore, does not affect the solution appreciably.

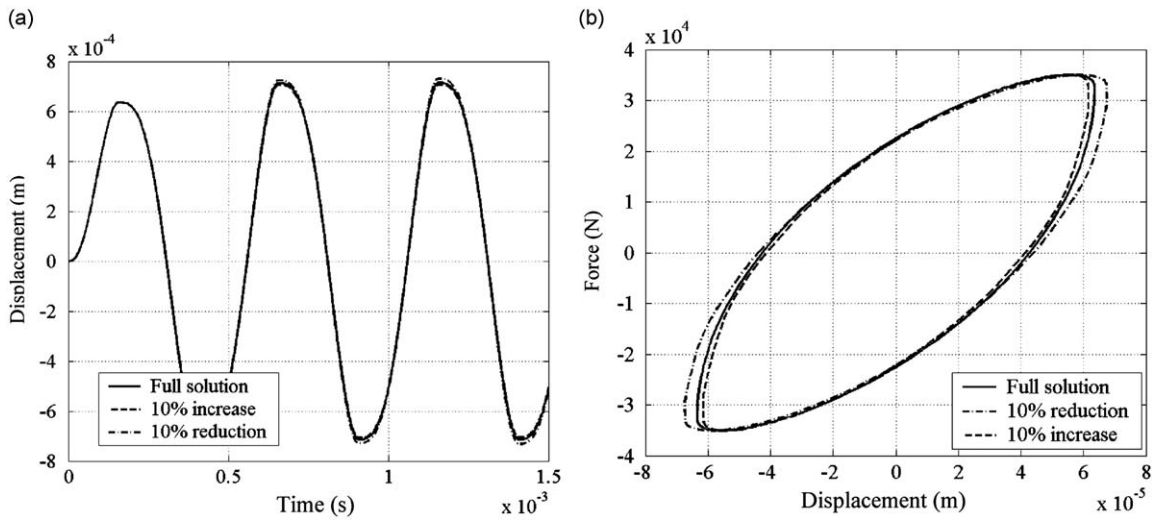

Fig. 11. Sensitivity of the response to change in the value of active length: (a) displacement; and (b) force-deflection behaviour (curves are overlapping).

Table 4
Sensitivity of the response on the change in the value of active length (Fig. 11).

Analysis type	Max. displacement (m)	Energy/cycle (J)
Dynamic FE analysis (full)	5.7×10^{-5} (0%)	681 (0.0%)
10% increase in active length	7.06×10^{-4} (1.1%)	672 (1.3%)
10% reduction in active length	7.3×10^{-4} (2.2%)	691 (1.5%)

7. Application of the method to different systems

After having developed a procedure for the reduction of the size of the joint model and the determination of the active length of the joint beforehand, different systems are analysed. These systems are essentially models of a joint subjected to different excitation conditions.

7.1. Harmonic excitation applied to an isolated joint

Using the POMs obtained from the analysis of the reference system, various cases of an isolated joint are analysed. System parameters and the excitation force and frequency for these cases are given in Table 5. The excitation frequency is selected to be in the vicinity of the resonance of the system except for Case VI in which the excitation frequency is well below the system resonance.

Table 5
Structure parameters and loading conditions for various cases in Figs. 12 and 13.

Parameter	Case IV	Case V	Case VI	Case VII
Joint length (mm)	250	300	400	500
Plate thickness (mm)	10	10	10	10
First resonance (Hz) (half length)	10000	8333	6250	5000
F_{exc} (kN)	35	35	35	35
f_{exc} (Hz)	10000	8000	60	5000

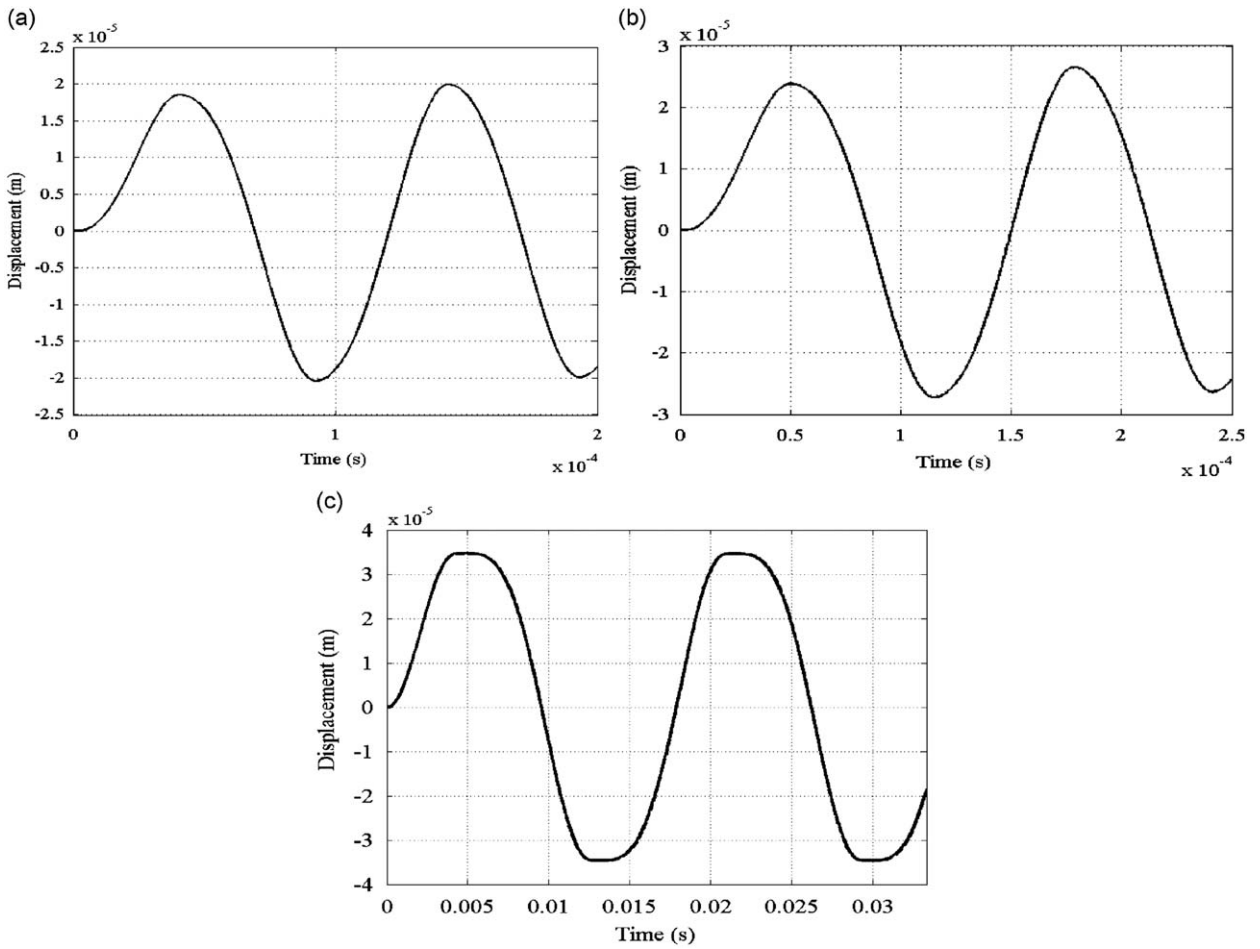

Fig. 12. Comparison of the time histories of the displacements at the free end of the joint for full (solid curve) and reduced (dashed curve) systems: (a) Case IV; (b) Case V; and (c) Case VI. Curves are overlapped.

A comparison of the displacement time history for the full and reduced-order models for the three different cases is shown in Fig. 12. These displacements correspond to the node at the free end of the joint. Fig. 12(a) shows a comparison between full and reduced systems for Case IV using five POMs. The solid and dashed curves correspond, respectively, to the full and reduced model. These two curves overlie each other almost exactly. The same is true for Figs. 14(b) and (c) showing the comparison for Cases V and VI, respectively.

The percentage error in displacement of the reduced system for Case VII is shown in Fig. 13 and it is <2 percent. The error is plotted for one case only as in other cases the difference between full and reduced models is hardly noticeable. Fig. 12(a) and (b) do not show the stick slip behaviour very clearly. This is because the frequency of excitation is selected in the vicinity of the system resonance. The stick-slip behaviour can be observed for the third case only which is obtained for excitation with low frequency. A clearer picture of the stick-slip behaviour is shown in Fig. 14. This figure shows that nodes away from the free end of the joint experience well-defined stick-slip behaviour. The four points selected for this figure are equally spaced along the length of the joint.

7.2. Impulsive excitation applied to an isolated joint

So far the various cases studied are concerned with harmonic excitations and they are relatively straightforward. Since a system containing joints can be subjected to excitation conditions that are not necessarily a harmonic one, the procedure needs to be investigated in case of more general excitation conditions. Impulsive excitation is one such case.

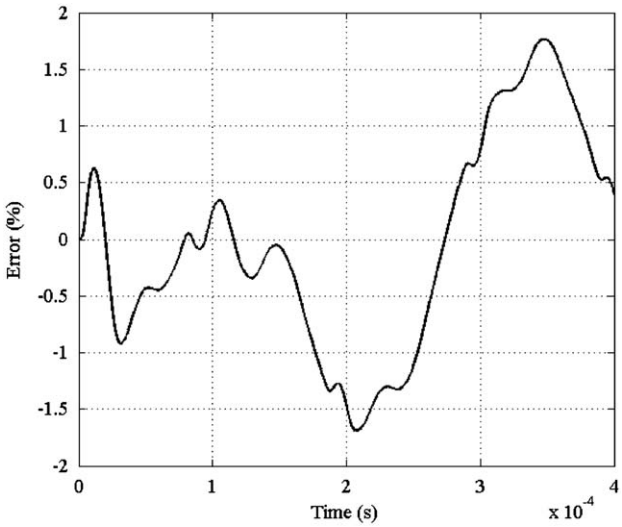

Fig. 13. The percent error (compared with full solution) for Case VII.

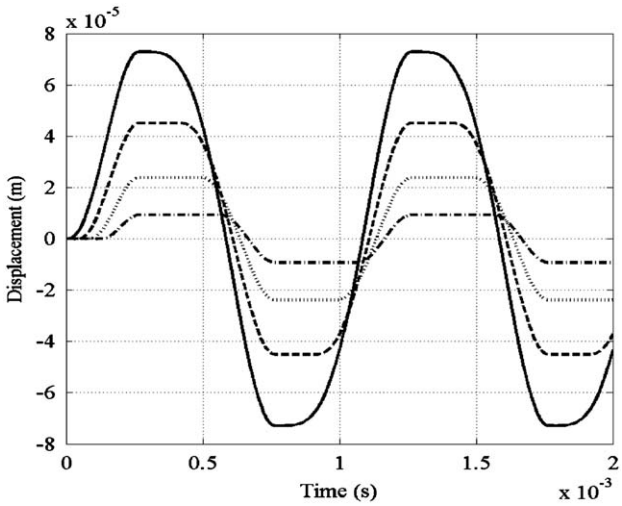

Fig. 14. Stick-slip behaviour of four equally spaced nodes along the length of the joint.

In this section, an impulse input is used to excite the system. Parameters of the impulse input, i.e. the amplitude and the frequency contents are selected so as to excite several internal resonances of the system. The geometry of the system in Case VII is selected for this purpose. A zoomed view of the impulse is shown in Fig. 15. The amplitude of the impulsive input is selected as 50 percent of the friction limit of the joint to make sure that at least 50 percent of the joint length is active. Assume that the system length is 250 mm (50 percent of 500 mm). The extensional resonances for this length are odd-multiples of 5000, i.e. 5000, 15 000 and 25 000 Hz, etc. As can be seen from Fig. 15, the time for the force to reach to its peak value is 2×10^{-5} s which can capture frequencies up to and including 25 000 Hz. According to the Nyquist rule the value of the time interval should be $1/2f_{exc}$ in order to capture f_{exc}. As the system has a softening behaviour, the first three internal resonances of this system will, however, be lower than the maximum frequency present in the excitation.

The first five POMs obtained from the time history of the transient response are shown in Fig. 16. These POMs are plotted against the length of the joint (grey plus active) and they show that for excitation amplitude of 50 percent of the friction limit, the active length is almost 82 percent, suggesting that inertia effects are present. The cumulative sum for the first five PVs is slightly higher than 99 percent of the total. This suggests that five POMs should be used in the model reduction of this system. The shape of the POMs in the active region looks quite similar to the ones obtained for harmonic excitation, Fig. 5, except for the first one that contributes around 80.6 percent to the total sum of the PVs. The response at the free end of the joint using the full system and reduced system is plotted in Fig. 17(a) with a zoomed view in Fig. 17(b). The various cases analysed are denoted (i) full system, (ii) reduced system using five POMs obtained from the impulse

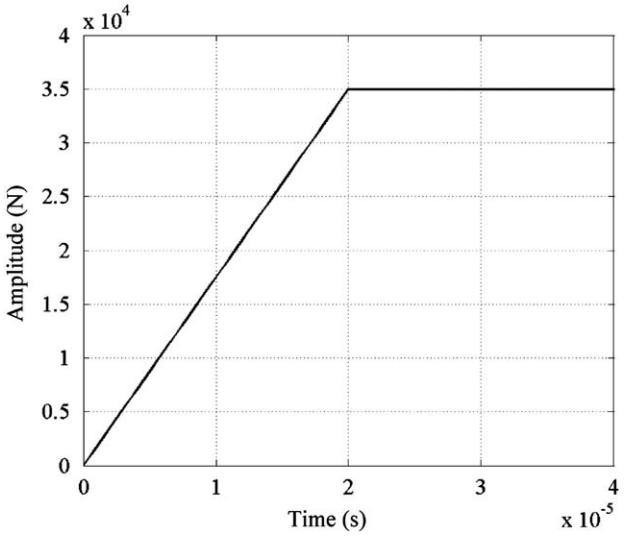

Fig. 15. Zoomed view of the impulse.

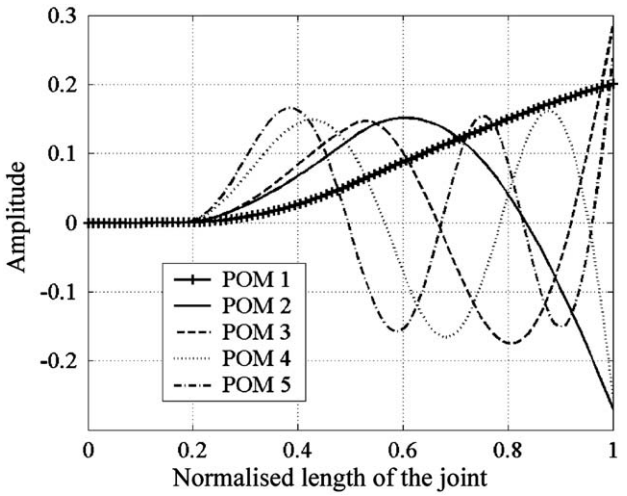

Fig. 16. First five POMs for the step input case.

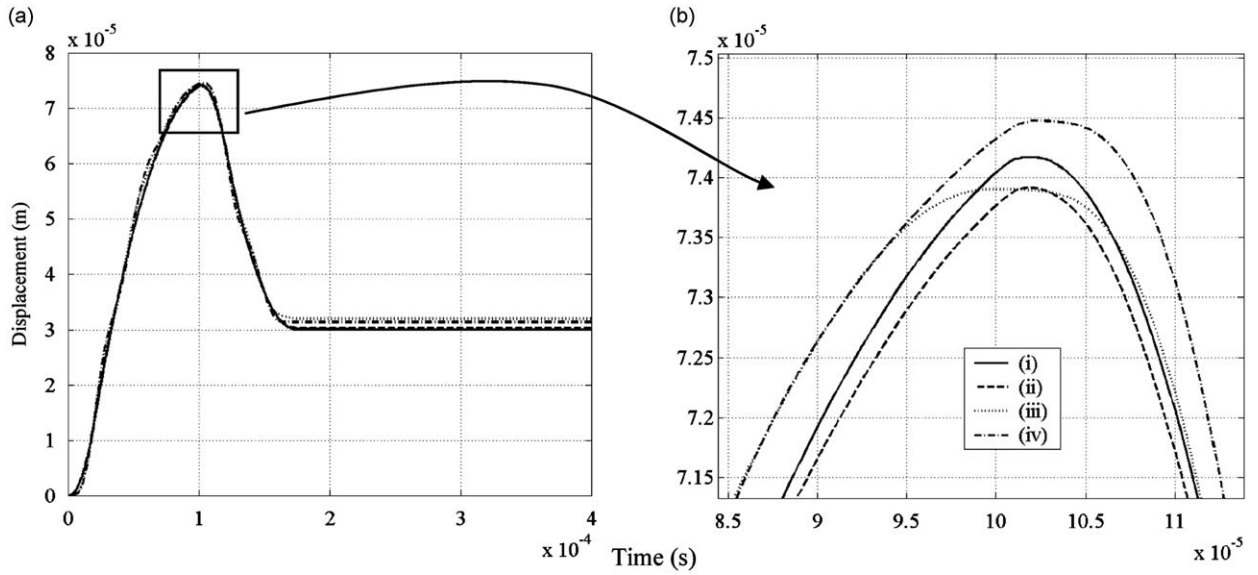

Fig. 17. Response of joint to step excitation: (a) complete time history; and (b) zoomed view of (a). (i) Full system; (ii) reduced system using five POMs obtained from impulsive excitation; (iii) same as (ii) but with 11 POMs and (iv) reduced system using five POMs obtained from harmonic excitation.

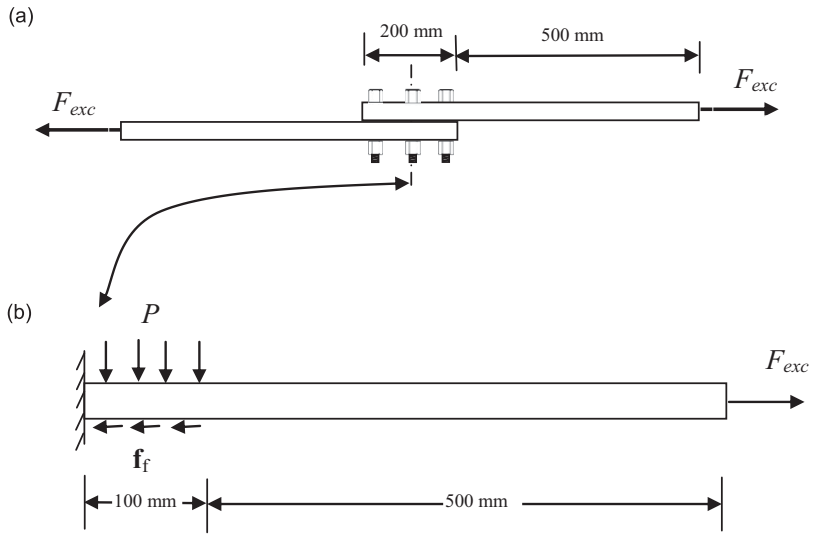

Fig. 18. Structure with a joint: (a) actual system; and (b) its simplified model.

response of the system, (iii) same as (ii) but with 11 POMs and (iv) using five POMs obtained from the response of the system to harmonic excitation. The error in any case is <1 percent. This suggests that the POMs obtained using the harmonic excitation can be used to reduce the dynamics of a joint subjected to impulse excitation. This is a very important result.

The case of excitations at frequencies between any two system resonances can also be handled with the same method used for the impulsive excitations because it is again very difficult to determine the active length for excitations at more than one frequency. A straightforward reason is the lack of validity of the superposition principal for the joint dynamics.

7.3. Harmonic excitation applied to a jointed structure

The jointed structure consists of two plates, each of size $700 \times 50 \times 10$ mm. The joint is formed by clamping the two plates with an overlapping length of 200 mm, see Fig. 18(a). A simplified model of the joint consists of a plate of size $600 \times 50 \times 10$ mm with only 100 mm experiencing friction force. This model is obtained by exploiting the anti-symmetry in

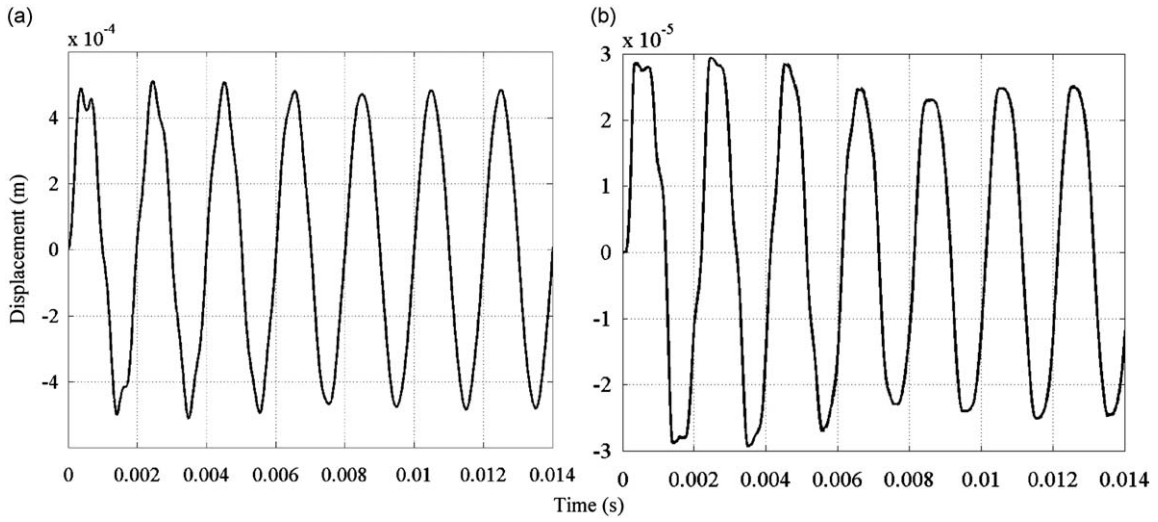

Fig. 19. Time histories of displacement for full (solid) and reduced (dashed) solution: (a) at the free end of the linear region; and (b) at the junction of the nonlinear and linear regions. The solid and dashed curves are almost overlapped.

the original structure and assuming the lower plate to be rigid. The simplified representation of the structure is shown in Fig. 18(b).

The amplitude of the harmonic force is 50 percent of the friction limit and its frequency is 500 Hz. The clamping pressure is 50 MPa and the friction coefficient is 0.7. The active length of the joint subjected to this level of excitation, without considering the inertia effects, is 50 percent of the joint region (100 mm), i.e. it is 50 mm. This means that the length of the structure experiencing displacement is 550 mm. The first resonance of a plate of this length is at around 2273 Hz. This value is well above the excitation frequency of 500 Hz.

The active length is scaled by a factor A_a according to (4) to include the inertia effects of the portion of the structure that experiences motion. This value comes out to be 1.05, which means that the active length is 1.05×50 percent $\sim$53 percent of the 100 mm length.

The system response for the full and reduced-order models is shown in Fig. 19. Fig. 19(a) shows the displacement at the free end of the linear region, while Fig. 19(b) shows the displacement at the junction of the nonlinear and the linear regions. The difference in displacements is hardly noticeable and is <1 percent of the response of the full system. The error at the junction is slightly higher than 1 percent during the transient phase of the solution but is lower than 1 percent during the steady state.

The steady-state energy dissipation in the joint region per cycle is the sum of energy dissipated at each node due to friction. The values of the dissipated energies are 3.08 and 3.3 J for the full and reduced model, respectively. The error in energy dissipation for the reduced model is, therefore, 8 percent of the value obtained for the full model. Although the error in the dissipation of energy seems large, it seems to be acceptable due to the fact that joint model is solved using only five POMs that were determined from the dynamics of the reference system which is an entirely different system in terms of the excitation and geometry.

7.4. *Impulsive excitation applied to a jointed structure*

The method is now applied to the structure of Fig. 18(b) excited by an impulse. The impulse is shown in Fig. 20. The maximum amplitude of the impulse is 50 percent of the friction limit of the joint. The time for the impulse to reach its maximum value is selected to be 4×10^{-5} s. This value is small enough to excite at least the first three resonances of the structure significantly. The third resonance of the structure at 50 percent load amplitude is 11 365 Hz which is the third odd-multiple of the first resonance at 2273 Hz. This suggests a value of $1/2 \times 11\,365 = 4.4 \times 10^{-5}$ s (applying the Nyquist rule) for the rise time of the impulse. A slightly smaller value, 4×10^{-5} s, is selected to be on the safe side.

The time histories of the full and reduced models are plotted in Fig. 21 and they are showing very good agreement. The maximum error in the nodal displacement between the full and reduced models at the free end of the structure and the interface of the linear and nonlinear regions is 2.3 percent and 1.5 percent, respectively. It should be noted that the decay envelope of the response does not follow the well-known linear decay behaviour. This is due to the magnitude of friction forces which are comparable to the elastic forces in the joint. This behaviour is also observed in [17]. The linear decay behaviour is observed in systems which have smaller friction forces compared with the elastic forces, see for example [11].

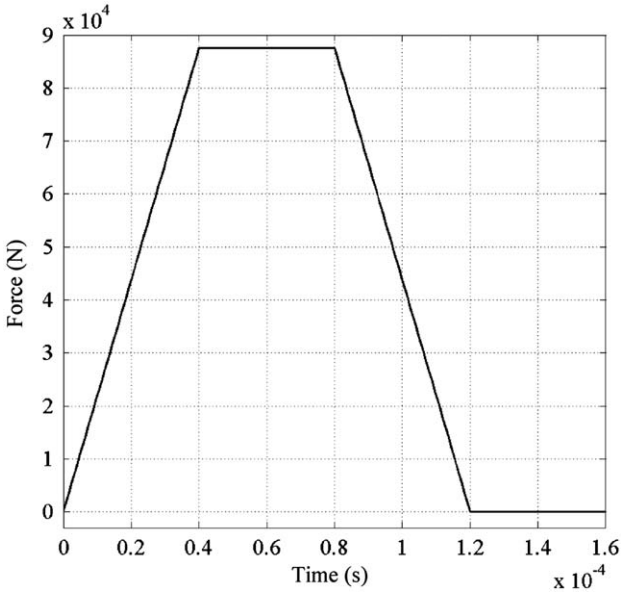

Fig. 20. Time history of the impulsive force.

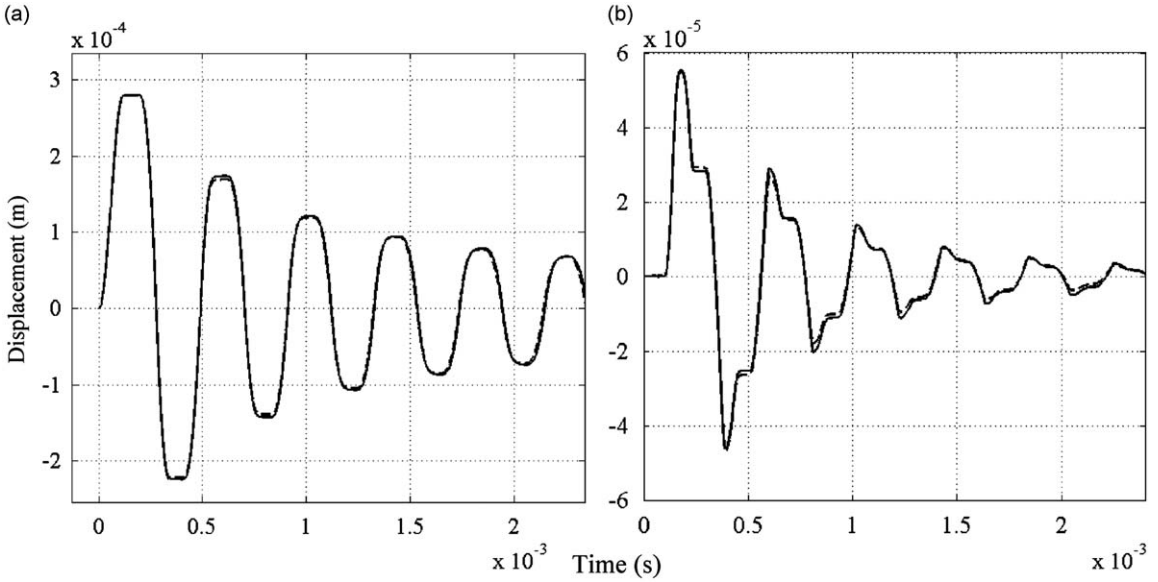

Fig. 21. Time histories of displacement for full (solid) and reduced (dashed) solution for impulsive excitation: (a) at the free end of the linear region; and (b) at the junction of the nonlinear and linear regions. The solid and dashed curves are almost overlapped.

7.5. Evaluating the computational advantage of the model reduction

The main advantage in computational time is obtained from an increase in the size of the stable time step as only the linear part of the model is reduced without reducing the number of nonlinear functions. The ratio of the length of the stable time step size for the reduced and full model is inversely related to the ratio of their maximum eigenvalues, which is a factor of around 17 for joints studied in this paper.

It is known that the number of arithmetic operations required for the determination of the acceleration vector for a banded system of size n is of the order n or $O(n)$, while for a system with full matrices of size n, it is $O(n^2)$ when the LU decomposition is employed. The matrices obtained in the paper for the reduced models, having j generalised coordinates, are fully populated and hence require arithmetic operations of $O(j^2)$. In addition $O(n)$ operations are required for the determination of the vector of nonlinear forces. The coefficient of n in the expression for total number of computations is, however, small compared with that for a banded system. This is explained in the next paragraph.

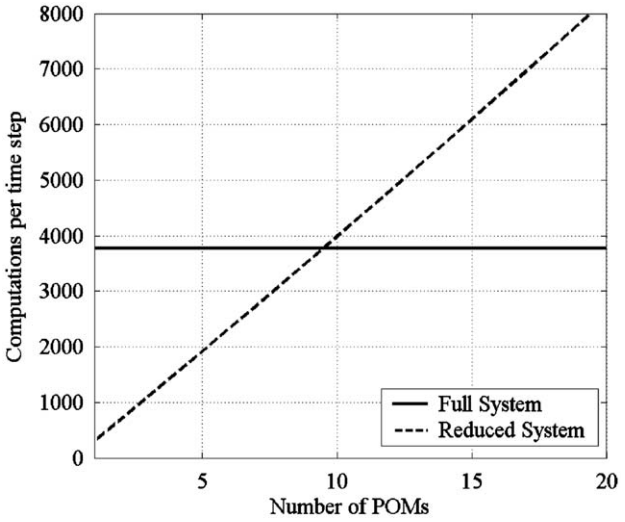

Fig. 22. Variation of number of computations per time step to determine the rate vector.

While determining the second half of the rate vector, which is acceleration of the generalised coordinates, one needs a total of $38n-24$ operations per time step. Here, n is the number of generalised coordinates in the full system that is equal to 100. This means that a total of about 3800 computations are required. On the other hand, for the reduced system, one needs a total of $4nj-n-j$ computations for the expansion and compression phase and j^2-j computations for the determination of the second half of the rate vector. The sum of these computations is around 1900. This shows a 50 percent reduction in computational time during the determination of the rate vector. This saving is, however, lost when the number of POMs is increased above nine. This can be seen from Fig. 22, where one has the number of computations per time step as a function of the number of POMs. The number of coordinates in the full system is fixed to 100. The horizontal line shows the number of operations for the full system while the slant line shows the computations for the reduced system.

8. Conclusions

A model of the joint dynamics is developed which is parameter-free and physics-based and capable of modelling shear lap joints with reasonable accuracy. The method can be applied to different levels of loading and different joint parameters, e.g. different joint geometry, friction coefficients and clamping pressures. The inertia effects in the joint, which are usually ignored, are automatically included in the formulation. The dynamics of both isolated joints and jointed structures can be simulated with accuracy for various excitation conditions.

An important feature of the method is the determination of the active length of a joint which is then used to properly scale out the proper orthogonal modes. The active length can be determined easily for harmonic excitations in the sub-resonance range.

The method reduces the linear part of the system of equations. This results in a reduction in computational time in terms of the increase in the size of the stable time step. This size is usually increased by a factor in excess of 10. The reduction in computational time is also obtained by the lower number of coordinates for the integration phase of the solution.

Acknowledgements

I would also like to thank my department, National Centre for Physics, Pakistan for the financial support for the first two years of my research and the School of Mechanical, Materials, and Manufacturing Engineering, the University of Nottingham, for the financial support for the third year of my study.

References

[1] C.F. Beards, Damping in structural joints, *Shock and Vibration Digest* 24 (1992) 3–7.
[2] A.F. Metherell, S.V. Diller, Instantaneos energy dissipation rate in a lap joint: uniform clamping pressure, *Journal of Applied Mechanics* (1968) 123–127.
[3] D.D. Quinn, D. Segalman, Using series–series Iwan type models for understanding joint dynamics, *Transactions of the ASME, Journal of Applied Mechanics* 72 (2005) 666–673.

[4] G. Csaba, Modelling Microslip Friction Damping and its Influence on Turbine Blade Vibrations, Ph.D. Thesis, Linköping University, 1998.
[5] L. Gaul, J. Lenz, Nonlinear dynamics of structures assembled by bolted joints, *Acta Mechanica* 125 (1997) 169–181.
[6] M. Oldfield, H. Ouyang, J.E. Mottershead, A. Kyprianou, Modelling and simulation of bolted joints under harmonic excitation, *Materials Science Forum* 440–441 (2003) 421–428.
[7] D.W. Lobitz, D.L. Gregory, D.O. Smallwood, Comparison of finite element predictions to measurements from the Sandia microslip measurement. *Proceedings of the IMAC XIX*, Orlando, 2001, pp. 1388–1394.
[8] M.V. Sivaselvan, A.M. Reinhorn, Hysteretic models for deteriorating inelastic structures, *Journal of Engineering Mechanics—ASCE* 126 (2000) 633–640.
[9] D. Segalman, Modelling joint friction in structural dynamics, *Structural Control and Health Monitoring* 13 (2006) 430–453.
[10] P. Holmes, J.L. Lumley, G. Berkooz, *Turbulence, Coherent Structures, Dynamical Systems, and Symmetry*, Cambridge University Press, Cambridge, 1996.
[11] D.J. Inman, *Engineering Vibration*, Prentice-Hall, New Jersey, 2003.
[12] R.I. Leine, D.H. Van Campen, A. De Kraker, L. Van Den Steen, Stick-slip vibrations induced by alternate friction models, *Nonlinear Dynamics* 16 (1998) 41–54.
[13] G. Strang, *Linear Algebra and its Applications*, Thomas Learning Inc., 1988.
[14] Matlab, *Using Matlab Version 6*, The Mathwork Inc, MA, 2000.
[15] A.R. Khattak, Dynamic Characteristics of Bolted Joints, Ph.D. Thesis, University of Nottingham, Nottingham, 2006.
[16] S.H. Crandall, The role of damping in vibration theory, *Journal of Sound and Vibration* 11 (1970) 3–18.
[17] C.J. Hartwigsen, Y. Song, D.M. McFarland, L.A. Bergman, A.F. Vakakis, Experimental study of non-linear effects in a typical shear lap joint configuration, *Journal of Sound and Vibration* 277 (2004) 327–351.